

RESEARCH

Open Access



Spatial and morphologic features of lenses with different axial lengths in cataract patients: a swept-source optical coherence tomography-based study

Chao Chen^{1,2,3†}, Jiaqi Meng^{1,2,3†}, Kaiwen Cheng^{1,2,3†}, Ching Kang^{1,2,3}, Liguang Zhou^{4*†}, Haike Guo^{5*†} and Xiangjia Zhu^{1,2,3,6*†}

Abstract

Background To investigate the spatial and morphologic features of lenses with different axial length (ALs) in cataract patients using swept-source optical coherence tomography (SS-OCT).

Methods Totally 105 eyes of 105 patients scheduled to have cataract surgery were included. Eyes were divided into the control (AL < 24.5 mm), moderate myopia (MM, 24.5 ≤ AL < 26 mm) and high myopia (HM, AL ≥ 26 mm) groups. Spatial features including lens vault (LV) and iris-to-lens distance (ILD), and morphologic features including radii of curvature of anterior and posterior surface (Ra, Rp), lens diameter (LD) and lens thickness (LT) were measured in eight directions by SS-OCT.

Results Spatially, the HM group had larger LV and ILD than the control group (both $P < .05$). LV and ILD were negatively correlated with AL, respectively (LV: $r = -.484, P < .0001$; ILD: $r = -.656, P < .0001$). Morphologically, both MM and HM groups had greater Ra and Rp than the control group. Ra was positively correlated with AL ($r = .622, P < .0001$), while the relationship between Rp and AL was non-linear. Moreover, the MM and HM groups had larger LD than the control group (both $P < .001$). Anterior LT was thinner in the HM than in the MM group ($P = .026$), while posterior LT between these two groups was similar. When compared in eight directions, similar trends were seen in Ra, Rp and LD, and the HM group showed a greater difference in Ra between horizontal and vertical directions.

[†]C. Chen, J. Meng and K. Cheng contributed equally as co-first authors.

[†]L. Zhou, H. Guo and X. Zhu contributed equally as co-last authors.

*Correspondence:

Liguang Zhou
zhouliguang1982@163.com
Haike Guo
guohaike@hotmail.com
Xiangjia Zhu
zhuxiangjia1982@126.com

Full list of author information is available at the end of the article



Conclusions This SS-OCT-based study showed that longer axial length is associated with a flatter lens, which was mainly attributed to the increase of Ra and LD. Longitudinal studies would be necessary to establish a causal relationship and temporal progression.

Keywords Axial length, Cataract, Lens morphology, Lens position, SS-OCT

Background

Modern cataract surgery has entered the refractive cataract surgery era with the advancement of phacoemulsification and intraocular lens (IOL) design [1–3]. Understanding the spatial and morphologic features of lenses can help to know the factors associated with the quality of postoperative refractive outcome, such as actual lens position of IOL and the compatibility between IOL and capsular bag [4–7]. Despite the rapid development of cataract surgery, previous studies on the spatial and morphologic features of lenses have remained limited to the parameters that can be directly measured by the current biometric instruments, such as anterior chamber depth (ACD) and lens thickness (LT) [8–10], which are closely related to axial length (AL) [11, 12]. However, more detailed parameters, including lens vault (LV), and radii of curvature of anterior and posterior lens surfaces (Ra and Rp), have not been sufficiently studied due to technical limitations, let alone the relationship between these parameters and AL.

The purpose of this study was therefore to investigate the spatial and morphologic features of lenses with different ALs in cataract patients based on swept-source optical coherence tomography (SS-OCT).

Materials and methods

Subjects

In this cross-sectional study, we included eyes that scheduled to undergo cataract surgery between March and December 2023 at the Eye and Ear, Nose and Throat (EENT) Hospital of Fudan University. The study was approved by the Institutional Review Board of the Eye and Ear, Nose, and Throat Hospital of Fudan University, Shanghai, China (approval reference number: 2020005), and adhered to the tenets of the Declaration of Helsinki. It was affiliated with the Shanghai High Myopia Study launched at the EENT Hospital of Fudan University since 2015 (www.clinicaltrials.gov, NCT03062085). Written informed consents were obtained from all participants for participation in the study and the use of their medical information for study analyses. To ensure the comparability, only eyes with cortical, nuclear or posterior subcapsular opacification graded 2 or 3 based on Lens Opacity Classification System III (LOCS III) were included. No significant difference was found between three groups in the grading of each type of opacification (Table 1). Eyes were excluded if they had a history of zonular weakness, glaucoma, uveitis, corneal opacity,

iris abnormalities, severe fundus pathologies, strabismus, previous trauma or ocular surgery, or low imaging quality. Severe fundus pathologies included macular atrophy, choroidal neovascularization, and myopic maculopathy grading >3 defined by META-PM classification system [13], etc., which may confound the result or affect the patient's cooperation during examination. Imaging quality was assessed by image score provided by built-in software of OCT instrument, and the image with a score lower than 9 was regarded as low quality. For patients with both eyes planned to have cataract surgery and meeting the inclusion criteria, only one eye was randomly selected. Finally, 105 eyes of 105 patients were included and divided into three groups according to AL: the control (AL < 24.5 mm, $n=48$), moderate myopia (MM, $24.5 \leq AL < 26$ mm, $n=28$) and high myopia (HM, $AL \geq 26$ mm, $n=29$) groups.

Ophthalmic examinations

Routine ophthalmic examinations were conducted on each eye, including assessment of visual acuity, intraocular pressure (IOP), slit-lamp examinations, funduscopy, IOLMaster 700 (Carl Zeiss AG, Oberkochen, Germany), corneal topography (Pentacam HR; Oculus Optikgeräte GmbH, Wetzlar, Germany), B-scan ultrasonography, and fundus OCT. Each device was operated by an experienced examiner.

Anterior segment OCT data acquisition and data processing

Spatial and morphologic features of lenses were measured using a wide full-range SS-OCT (TowardPi Yalkaid, TowardPi Medical Technology, Beijing, China), with a wave length of 1,060 nm, a scanning speed of 100 kHz A-scans per second and an axial optical resolution of 3.8 μm . The images were captured in the dark. After dilating the pupil with a mixture of 0.5% phenylephrine and 0.5% tropicamide (1% Mydrin-P, Santen, Japan), the patient was told to stare at a fixation target to ensure the scan was centered on the corneal vertex. The SS-OCT measurement was then performed in eight scanning directions with 22.5° as the interval (Fig. 1A), and finally generated eight anterior segment images in one scan unit. For each image, the software built in the SS-OCT automatically fitted a complete mimic lens based on scanned anterior and posterior surfaces, and needed parameters could then be measured (Fig. 1B). The result of the software fitting the lens for each image was

Table 1 Patient characteristics

Parameter	Control (48 eyes)	Moderate myopia (28 eyes)	High myopia (29 eyes)	P value
Age, years	67.0±6.7	59.9±10.5	54.5±7.8	<0.001*
Sex, male/female	17/31	12/16	12/17	0.778
Eye laterality, right/left	30/18	14/14	19/10	0.436
AL, mm	23.01±0.60	25.13±0.43	28.14±1.52	<0.001*
Corneal power, diopters	44.46±1.14	43.07±1.52	42.49±2.70	<0.001*
ACD, mm	2.94±0.30	3.40±0.36	3.59±0.30	<0.001*
IOP, mm Hg	13.1±2.9	13.2±2.8	14.2±2.7	0.070
Cortical opacification, yes/no	17/31	9/19	4/25	0.112
Nuclear opacification, yes/no	41/7	24/4	25/4	>0.999
Posterior subcapsular opacification, yes/no	8/40	6/22	4/25	0.757

*Statistically significant ($P < .05$)

AL, axial length; ACD, anterior chamber depth; IOP, intraocular pressure

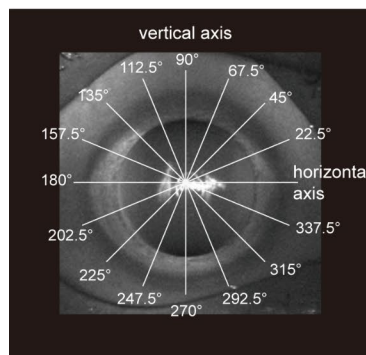
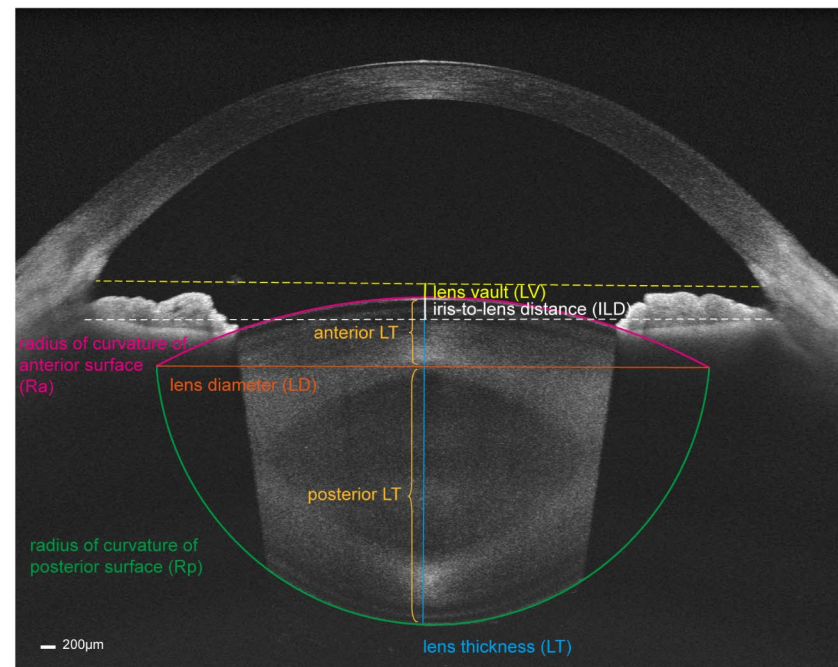
A**B**

Fig. 1 Measurement of spatial and morphologic features of lenses using swept-source optical coherence tomography (SS-OCT). **(A)** The SS-OCT measurements were performed in 8 scanning directions with 22.5° as the interval. **(B)** A complete lens shape was fitted by software built in instrument. Lens vault (LV, yellow line) was defined as vertical distance from the anterior lens vertex to the line connecting the scleral spurs. Iris-to-lens distance (ILD, white line) was defined as the vertical distance from the anterior lens vertex to the line connecting iris roots. Radii of curvature of anterior surface (Ra, red line) and posterior surface (Rp, green line) were measured by built-in software automatically. Lens diameter (LD, orange line) was defined as the length of line connecting the intersections of anterior and posterior curvatures on both sides. Lens thickness (LT, blue line) was defined as the length of line connecting the anterior and posterior lens vertex. Anterior LT (upper brown line) was defined as the distance from anterior lens vertex to the diameter line, and posterior LT (lower brown line) was calculated as LT minus anterior LT

manually checked. For images with poor fitting result, the fitting lines of anterior and posterior surfaces were manually adjusted through the software to get a good fitting result.

In terms of spatial features, lens vault (LV) and iris-to-lens distance (ILD) were measured. LV was defined as vertical distance from the anterior lens vertex to the line connecting the scleral spurs [14], and ILD was defined

as the vertical distance from the anterior lens vertex to the line connecting iris roots (Fig. 1B). The iris root was determined by the endpoint of the posterior edge of the iris near to the cornea. Positive values of LV or ILD indicated the lens vertex was anterior to the lines connecting scleral spurs or iris roots, while negative values indicated lens vertex was located posterior to the corresponding lines.

In terms of morphologic features, radius of curvature of anterior surface (Ra), radius of curvature of posterior surface (Rp), lens diameter (LD), lens thickness (LT), anterior LT and posterior LT were measured. Because the measurement was based on the fitted lens, Ra and Rp reflect the radius curvature of the central zone of lens surface. LD was defined as the length of line connecting the intersections of anterior and posterior curvatures on both sides (Fig. 1B) [15]. LT was defined as the length of line connecting the anterior and posterior lens vertex (Fig. 1B). Anterior LT was then defined as the distance from anterior lens vertex to the diameter line, and posterior LT was calculated as LT minus anterior LT (Fig. 1B).

Among these parameters, LV, Ra, Rp and LT were measured by software automatically. The relevant lines of remaining parameters were drawn manually and calculated using the tools built into the software. The average values of the parameters in the eight directions were firstly used to compare between three AL groups in the overall level. When the data for each direction were compared individually, the data of right and left eyes were combined under the rules that the scanning axes of right and left eyes were symmetric about the nasal septum, that is, they made complementary angles to the horizontal axis. The difference in Ra between horizontal axis (Ra0) and vertical axis (Ra90) was calculated as Ra0-Ra90 for each eye.

Statistical analysis

All continuous data were presented as mean \pm standard deviation (SD) and compared among three AL groups using analysis of variance (ANOVA), Kruskal-Wallis test or analysis of covariance (ANCOVA) with age as covariates. Bonferroni test was used for the post hoc comparison. Categorical data were compared among three AL groups using χ^2 test or Fisher's exact test. Pearson's correlation coefficient (r) and scatterplot were used to determine the relationships between the AL and LV, ILD and Ra. Scatterplot of Rp versus AL was created and fitted using GAM method. Circular plot presented the real data of LD collected from eight directions and these data points were smoothly connected by curves using the R "ggplot2" package. A two-sided P value $< .05$ was considered statistically significant. All analyses were performed using IBM SPSS 26.0 (Chicago, Illinois, USA). Graphs were illustrated using Prism 9 (GraphPad, La Jolla, California, USA) and R 4.3.0 (R Foundation for Statistical computing).

Results

Patients' characteristics

Patients' characteristics according to AL were presented in Table 1. Among the three groups, age, AL, corneal power and ACD were significantly different

(Kruskal-Wallis test for age and AL; ANOVA for ACD and corneal power; all $P < .001$). Age was therefore adjusted in the subsequent analyses. There were no statistically significant differences in terms of sex, eye laterality, IOP, and any type of opacification (χ^2 test for sex, eye laterality, and cortical opacification; Fisher's exact test for nuclear and posterior subcapsular opacification; Kruskal-Wallis test for IOP; all $P > .05$).

Spatial features of lenses with different ALs

The average LV of the HM group was -0.38 ± 0.24 mm, which was significantly lower than that of the control group (-0.10 ± 0.23 mm, ANCOVA with Bonferroni post hoc test, $P < .001$, Fig. 2A). Pearson's correlation analysis showed LV was negatively correlated with AL ($r = -.484$, $P < .0001$; Fig. 2B). Similarly, both MM and HM groups had a shorter ILD compared with the control group (control: 0.65 ± 0.22 mm; MM: 0.37 ± 0.20 mm; HM: 0.19 ± 0.24 mm; ANCOVA with Bonferroni post hoc test, both $P < .0001$; Fig. 2C). ILD was also negatively correlated with AL ($r = -.656$, $P < .0001$; Fig. 2D).

Morphologic features of lenses with different ALs

Both Ra and Rp showed significant differences among three groups (ANCOVA, both $P < .001$, Table 2). Specifically, Ra of the HM group was greater than that of other two groups (Bonferroni post hoc test, both $P < .05$; Table 2). Pearson's correlation analysis showed Ra was positively correlated with AL ($r = .622$, $P < .0001$; Fig. 3A). Rp of the HM group was significantly greater than that of the control group (Bonferroni post hoc test, $P < .0001$, Table 2), while no difference in Rp was found between the MM and HM groups (Bonferroni post hoc test, $P = .593$, Table 2). The relationship between Rp and AL was non-linear. As AL elongated, Rp increased initially and then basically stabilized (Fig. 3B).

ANCOVA with Bonferroni post hoc tests showed LD was greater in both MM and HM groups than in the control group (both $P < .001$, Table 2), while no difference in LD was found between the MM and HM groups ($P = .748$). In terms of LT, the LT of the HM group was smaller than that of the control group ($P = .035$, Table 2). When the LT was divided into anterior and posterior parts based on diameter line, anterior LT was found to be thinner in the HM group than in the MM group (1.13 ± 0.19 versus 0.96 ± 0.22 , Bonferroni post hoc test, $P = .026$, Table 2), whereas posterior LT between these two groups remained similar (Bonferroni post hoc test, $P > .99$, Table 2). Additionally, posterior LT was slightly thinner in the MM than in the control group, which was at the brink of significance (Bonferroni post hoc test, $P = .064$, Table 2).

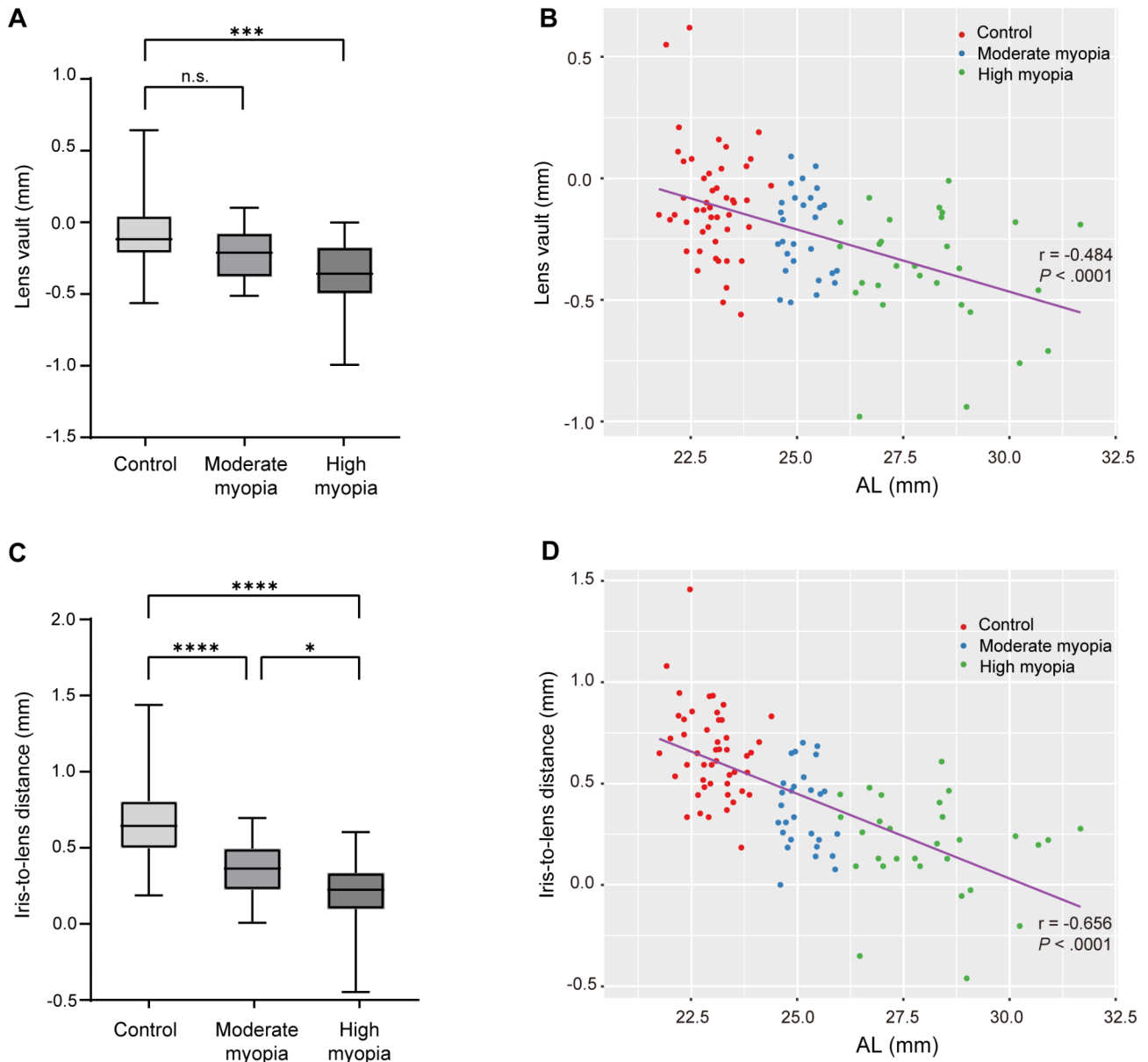


Fig. 2 Spatial features of lenses with different axial lengths (ALs). **(A)** Lens vault in three AL groups. $***P < .001$; n.s., not significant (analysis of covariance with Bonferroni post hoc test). **(B)** Lens vault was negatively correlated with AL ($r = -0.484, P < .0001$). **(C)** Iris-to-lens distance in three AL groups. $*P < .05$, $****P < .0001$ (analysis of covariance with Bonferroni post hoc test). **(D)** Iris-to-lens distance was negatively correlated with AL ($r = -0.656, P < .0001$)

Table 2 Morphologic features of lenses among three groups with different axial lengths

Parameter	Control (48 eyes)	Moderate myopia (28 eyes)	High myopia (29 eyes)	P value
Ra, mm	7.60 ± 0.82	8.58 ± 0.96	9.45 ± 1.34	< 0.001*
Rp, mm	3.96 ± 0.33	4.30 ± 0.39	4.42 ± 0.36	< 0.001*
LD, mm	7.77 ± 0.56	8.27 ± 0.56	8.41 ± 0.48	< 0.001*
LT, mm	4.69 ± 0.37	4.44 ± 0.45	4.24 ± 0.41	0.039*
Anterior LT, mm	1.10 ± 0.21	1.13 ± 0.19	0.96 ± 0.22	0.030*
Posterior LT, mm	3.59 ± 0.33	3.31 ± 0.39	3.28 ± 0.33	0.050*

*Statistically significant ($P < .05$)

AL, axial length; Ra, radius of curvature of anterior surface; Rp, radius of curvature of posterior surface; LD, lens diameter; LT, lens thickness

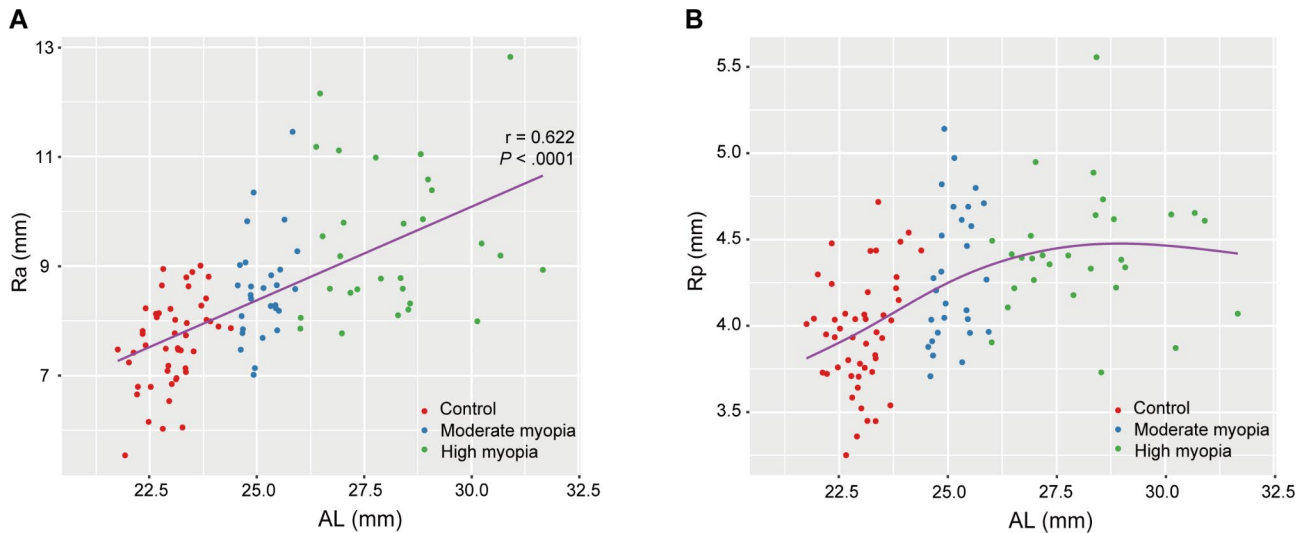


Fig. 3 Relationship between axial length (AL) and radii of curvature of anterior surface (Ra) or posterior surface (Rp). **(A)** Ra was positively correlated with AL ($r = .622$, $P < .0001$). **(B)** Scatterplot with GAM curve showed non-linear relationship between AL and Rp

Morphologic features of lenses in different directions

The morphologic features of lenses in different directions were shown in Fig. 4. Generally, compared with the control group, Ra, Rp and LD were greater in both MM and HM groups in all of the eight directions (ANCOVA with Bonferroni post hoc test, all $P < .05$, Fig. 4A to C). There were also significant differences in Ra between the MM and HM groups in most directions (ANCOVA with Bonferroni post hoc test, all $P < .05$, Fig. 4A), except for Ra in vertical axis (ANCOVA with Bonferroni post hoc test, $P = .42$, Fig. 4A). Further, HM group showed a larger difference in Ra between horizontal and vertical directions, as Ra0-Ra90 was significantly greater in the HM group than in the control and MM groups (ANCOVA with Bonferroni post hoc test, $P = .0501$ and 0.024 , respectively, Fig. 4D).

Discussion

The spatial and morphologic features of lenses are key factors in achieving desired post-operative refractive outcomes for cataract patients [16–18]. However, some important parameters, such as the LV, Ra, and Rp, and how they change with AL has not been fully studied yet. To overcome these issues, we used SS-OCT to comprehensively evaluate these lenses features and their relationships to AL in cataract patients.

With the elongation of AL, the amount of lens located posterior to the plane of the scleral spurs or iris roots became larger. We found both LV and ILD were negatively correlated with AL. LV was an indicator of lens position and has been found to have influence on the accuracy of IOL power calculation formulas in shallow anterior chamber eyes previously [14, 19, 20]. Similar effect of LV may also be found in long eyes, which

requires to be further investigated. We also defined a novel parameter of ILD measured as vertical distance from the lens vertex to the line connecting iris roots. Our results showed that ILD seemed to be more sensitive than LV in capturing the spatial changes of lens with AL ($r = -.656$ for ILD versus $r = -.484$ for LV). Considering the critical role of lens-position-associated parameters in the accuracy of IOL power calculation formulas, our data suggested further optimization of IOL formulas may incorporate these unconsidered parameters, which, admittedly, requires further research.

Interestingly in this study, we found longer axial length is associated with a flatter lens. This conclusion was consistent with previous studies [21, 22], but we conducted a more detailed exploration based on a relatively large sample. We found Ra was positively correlated with AL, while the relationship between AL and Rp was non-linear. Moreover, MM and HM groups had a larger LD than the control group. These results suggested that as AL elongated, the anterior surface of lens may keep flattening; meanwhile the posterior surface of lens first flattened and then stabilized. The flattening of lens was mainly attributed to the increase of Ra and the enlargement of LD. The LD in our study appeared to be somewhat smaller compared with previous studies [4, 23], possibly because the fitting of the lens was based on the central curvature of both lens surfaces that might be steeper than the periphery parts. Nonetheless, its change with the increase of AL was observed under the same measurement conditions. As to the change of LT, a thinner LT was observed in HM group, which was consistent with previous studies [24–26]. Moreover, the thinning of anterior LT with AL supports the changing trend of Ra, whereas posterior LT remained similar between the HM and MM groups,

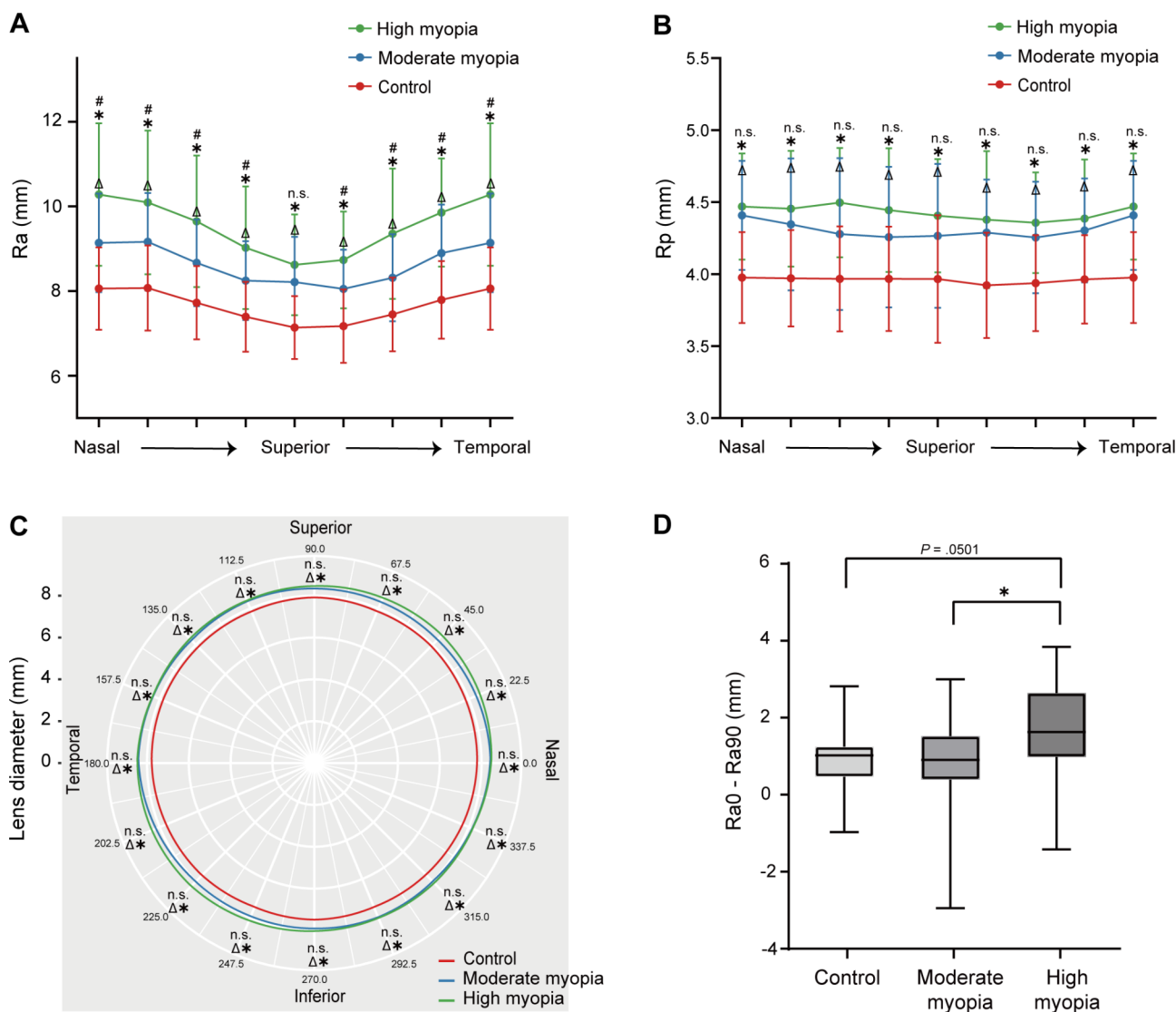


Fig. 4 Morphologic features of lenses in eight directions. **(A)** radii of curvature of anterior surface (Ra) and **(B)** posterior surface (Rp) in eight directions among three axial length (AL) groups. **(C)** Circular plot of lens diameter presenting the real data collected from eight directions with data points smoothly connected by curves using the R “ggplot2” package. For **(A)**, **(B)** and **(C)**: *comparisons between high myopia and control groups, $P < .05$; Δ comparisons between moderate myopia and control groups; n.s., not significant. **(D)** Difference values of Ra in horizontal axis (Ra0) minus Ra in vertical axis (Ra90) in three different AL groups. * $P < .05$. All data in this figure were analyzed using analysis of covariance with Bonferroni post hoc test

which reconfirmed that the anterior surface may act as the main factor for the flattening of lens with AL (Fig. 5).

When further investigating the morphologic features of lenses in different directions, above changing trends generally maintained. It was notable that the difference of Ra between horizontal and vertical axis (Ra0-Ra90) was greater in the HM groups, suggesting the flattening trend of anterior lens surface was more pronounced in the horizontal direction as AL increased. Overall, it suggested that with the elongation of AL, the lens may change from a thick oblate spheroid to a flattened oblate spheroid, and finally turned into an oblate ellipsoid with a flatten horizontal curvature. Such a changing pattern may be related to the upregulated expression of crystallins, and altered

proliferation and alignment of lens fibers with the elongation of AL [4], which required further investigation.

Clinically, the unique morphologic change of lenses with AL, along with the directional heterogeneity of Ra in highly myopic eyes may be the factors to be considered when selecting and designing IOL in the future. For instance, due to greater LD, the capsular bag size of highly myopic eye is possibly larger. For these patients, functional IOLs with plate-haptic design may be more appropriate than IOLs with C-loop haptic design, as the former have no gap between the optic and haptics and may get greater support from the capsular bag through its four corners. This speculation was supported by the observation that plate-haptic multifocal IOLs (MfIOLs)

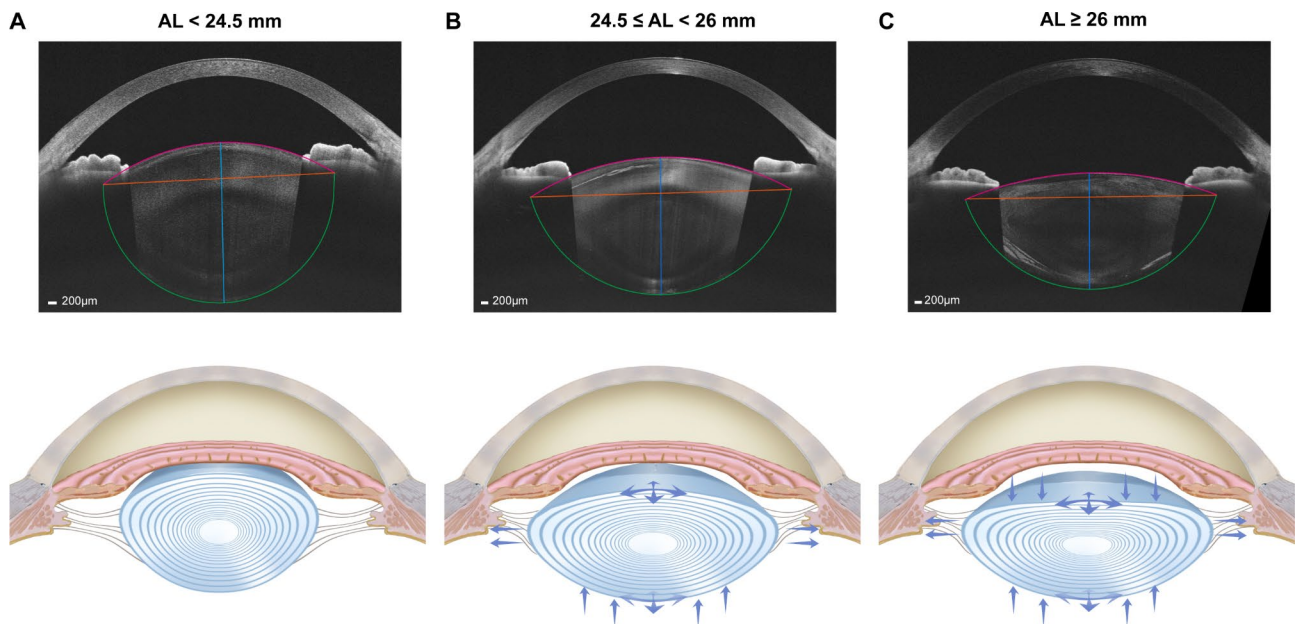


Fig. 5 Schematic diagram of lens changes as the axial length (AL) elongated. **(A)** A lens with a normal AL was shown ($AL < 24.5$ mm). **(B)** Moderate elongation of AL made the lens diameter (LD) get larger and posterior lens thickness (LT) get thinner, resulting in radii of curvature of anterior surface (R_a) and posterior surface (R_p) greater ($24.5 \leq AL < 26$ mm). **(C)** As AL further elongated, anterior LT got thinner, while the LD and posterior LT changed less, which made R_a get even greater while R_p show less change ($AL \geq 26$ mm)

showed less inferior decentration than C-loop haptic MfIOLs in highly myopic patients [5, 27]. In the future, designing functional IOLs that are more fitted for myopic eyes may improve postoperative outcomes better. Moreover, lens geometry is an important factor in IOL power calculation. When novel parameters, such as anterior LT, are incorporated into formula proposed recently, it was shown to improve the estimation of effective lens position (ELP) [28], a major source of error of IOL power calculation. Hence, development of IOL power calculation formulas incorporating more lens morphologic parameters may be a possible strategy to improve their predictive accuracy, especially for highly myopic eyes which possess unique lens morphologic features.

Besides AL, there are many other biometric parameters that are also related to the spatial and morphologic features of lenses. For instance, white-to-white (WTW) is an important parameter, which was positively correlated with R_a ($r = .212, P = .030$), R_p ($r = .360, P < .001$) and LD ($r = .318, P = .001$), and negatively correlated with LT ($r = -.202, P = .039$) and posterior LT ($r = -.292, P = .003$) in our data. These results provided preliminary insights into the association between WTW and lens features, and more investigations are warranted to exactly elucidate the relationships.

This study has several limitations that should be considered. First, the measurement approach in this study was based on the fitted lens, and the measurement of LD was based on the line connecting the intersections of anterior and posterior curvatures. Though being applied

in several previous studies [15, 24], the accuracy of this method should be further assessed. Second, owing to the cross-sectional design of this study, conclusions about the causality of AL on lens spatial and morphologic features could not be drawn, and a longitudinal approach would be necessary to establish a causal relationship and temporal progression. Third, the sample sizes of moderate and high myopia groups were relatively small, which we planned to increase in future studies to strengthen our findings. Fourth, the lack of external validation, ideally with different populations involved to confirm the generalizability of results, was another point that should be addressed in follow-up research.

Conclusions

In conclusion, based on the SS-OCT, we found that the longer axial length is associated with a flatter lens, which was mainly attributed to the increase of R_a and the enlargement of LD. Longitudinal studies would be necessary to establish a causal relationship and temporal progression. These data may help to the IOL selection and design for myopic cataract patients.

Abbreviations

ACD	Anterior chamber depth
AL	Axial length
ANCOVA	Analysis of covariance
ANOVA	Analysis of variance
ILD	Iris-to-lens distance
IOL	Intraocular lens
IOP	Intraocular pressure
LD	Lens diameter

LT	Lens thickness
LV	Lens vault
Ra	Radius of curvature of anterior surface
Rp	Radius of curvature of posterior surface
SS-OCT	Swept-source optical coherence tomography
WTW	White-to-white

Acknowledgements

Not applicable.

Author contributions

CC, JM and KC carried out the conception of the experimental idea, design of the methodology, collection and analysis of the data. CC draft the manuscript. CK was involved in data collection. XZ, HG and LZ reviewed and revised the manuscript. All authors read and approved the final manuscript.

Funding

This article was supported by research grants from the National Natural Science Foundation of China (82122017, 82271069, 82371040 and 81870642), Science and Technology Innovation Action Plan of Shanghai Science and Technology Commission (23Y11909800 and 21531904900), Outstanding Youth Medical Talents of Shanghai "Rising Stars of Medical Talents" Youth Development Program (2024420015).

Data availability

The data that support the findings of this study are available from the corresponding author upon reasonable request.

Declarations

Ethics approval and consent to participate

The study was approved by the Institutional Review Board of the Eye and Ear, Nose, and Throat Hospital of Fudan University, Shanghai, China (approval reference number: 2020005), and adhered to the tenets of the Declaration of Helsinki. It was affiliated with the Shanghai High Myopia Study launched at the EENT Hospital of Fudan University since 2015 (www.clinicaltrials.gov, NCT03062085). Written informed consents were obtained from all participants for participation in the study and the use of their medical information for study analyses.

Consent for publication

Not applicable.

Competing interests

The authors declare no competing interests.

Author details

¹Eye Institute and Department of Ophthalmology, Eye & ENT Hospital, Fudan University, Shanghai 200031, China

²NHC Key Laboratory of Myopia and Related Eye Diseases; Key Laboratory of Myopia and Related Eye Diseases, Chinese Academy of Medical Sciences, Shanghai 200031, China

³Shanghai Key Laboratory of Visual Impairment and Restoration, Shanghai 200031, China

⁴Department of Ophthalmology, Fenghua Hospital of Traditional Chinese Medicine, Ningbo 315500, Zhejiang, China

⁵Department of Ophthalmology, Shanghai Heping Eye Hospital, Shanghai 200437, China

⁶State Key Laboratory of Medical Neurobiology, Fudan University, Shanghai 200032, China

Received: 4 July 2024 / Accepted: 16 December 2024

Published online: 19 December 2024

References

- Du Y, Meng J, He W, et al. Challenges of refractive cataract surgery in the era of myopia epidemic: a mini-review. *Front Med (Lausanne)*. 2023;10:1128818. <https://doi.org/10.3389/fmed.2023.1128818>.
- Cicinelli MV, Buchan JC, Nicholson M et al. Cataracts. *Lancet* 2023; 401: 377–389. 20221221. [https://doi.org/10.1016/S0140-6736\(22\)01839-6](https://doi.org/10.1016/S0140-6736(22)01839-6)
- Lam D, Rao SK, Ratra V, et al. Cataract. *Nat Rev Dis Primers*. 2015;1:15014. <https://doi.org/10.1038/nrdp.2015.14>.
- Zhu X, Du Y, Li D, et al. Aberrant TGF-beta1 signaling activation by MAF underlies pathological lens growth in high myopia. *Nat Commun*. 2021;12:2102. <https://doi.org/10.1038/s41467-021-22041-2>.
- Zhu X, He W, Zhang Y, et al. Inferior decentration of multifocal intraocular lenses in myopic eyes. *Am J Ophthalmol*. 2018;188:1–8. <https://doi.org/10.1016/j.ajo.2018.01.007>.
- Plat J, Hoa D, Mura F, et al. Clinical and biometric determinants of actual lens position after cataract surgery. *J Cataract Refract Surg*. 2017;43:195–200. <https://doi.org/10.1016/j.jcrs.2016.11.043>.
- Qi J, He W, Zhang K, et al. Actual lens positions of three intraocular lenses in highly myopic eyes: an ultrasound biomicroscopy-based study. *Br J Ophthalmol*. 2022. <https://doi.org/10.1136/bjo-2022-322037>.
- Jonas JB, Nangia V, Gupta R, et al. Lens thickness and associated factors. *Clin Exp Ophthalmol*. 2012;40:583–90. <https://doi.org/10.1111/j.1442-9071.2012.02760.x>.
- Jonas JB, Nangia V, Gupta R et al. Anterior chamber depth and its associations with ocular and general parameters in adults. *Clin Exp Ophthalmol* 2012; 40: 550–556. 20120220. <https://doi.org/10.1111/j.1442-9071.2011.02748.x>
- Meng J, Wei L, He W, et al. Lens thickness and associated ocular biometric factors among cataract patients in Shanghai. *Eye Vis (Lond)*. 2021;8:22. <https://doi.org/10.1186/s40662-021-00245-3>.
- Sng CC, Foo LL, Cheng CY, et al. Determinants of anterior chamber depth: the Singapore Chinese Eye Study. *Ophthalmology*. 2012;119:1143–1150. <https://doi.org/10.1016/j.ophtha.2012.01.011>.
- Chen JH, Jiang WJ, Sun ZY, et al. Lens thickness and associated factors in Chinese children: the Shandong Children Eye Study. *Acta Ophthalmol*. 2017;95:e521–2. <https://doi.org/10.1111/aos.13431>.
- Ohno-Matsui K, Kawasaki R, Jonas JB, et al. International photographic classification and grading system for myopic maculopathy. *Am J Ophthalmol*. 2015;159:877–e883877. <https://doi.org/10.1016/j.ajo.2015.01.022>.
- Yan C, Yao K. Effect of Lens Vault on the Accuracy of Intraocular Lens Calculation Formulas in shallow Anterior Chamber eyes. *Am J Ophthalmol*. 2022;233(20210720):57–67. <https://doi.org/10.1016/j.ajo.2021.07.011>.
- Chen X, Gu X, Wang W, et al. Distributions of crystalline lens tilt and decentration and associated factors in age-related cataract. *J Cataract Refract Surg*. 2021;47:1296–301. <https://doi.org/10.1097/j.jcrs.0000000000000631>.
- Abdelghany AA, Alio JL. Surgical options for correction of refractive error following cataract surgery. *Eye Vis (Lond)* 2014; 1: 2. 20141016. <https://doi.org/10.1186/s40662-014-0002-2>
- Kieval JZ, Al-Hashimi S, Davidson RS, et al. Prevention and management of refractive prediction errors following cataract surgery. *J Cataract Refract Surg*. 2020;46:1189–97. <https://doi.org/10.1097/j.jcrs.0000000000000269>.
- Alio JL, Plaza-Puche AB, Fernández-Buenaga R, et al. Multifocal intraocular lenses: an overview. *Surv Ophthalmol*. 2017;62:611–634. <https://doi.org/10.1016/j.survophthal.2017.03.005>.
- Kim YC, Sung MS, Heo H, et al. Anterior segment configuration as a predictive factor for refractive outcome after cataract surgery in patients with glaucoma. *BMC Ophthalmol*. 2016;16:179. <https://doi.org/10.1186/s12886-016-0359-1>.
- Seo S, Lee CE, Kim YK, et al. Factors affecting refractive outcome after cataract surgery in primary angle-closure glaucoma. *Clin Exp Ophthalmol*. 2016;44:693–700. <https://doi.org/10.1111/ceo.12762>.
- Shang J, Hua Y, Wang Y, et al. Comparison of lens refractive parameters in myopic and hyperopic eyes of 6-12-year-old children. *Front Med (Lausanne)*. 2022;9:942933. <https://doi.org/10.3389/fmed.2022.942933>.
- Muralidharan G, Martinez-Enriquez E, Birkenfeld J, et al. Morphological changes of human crystalline lens in myopia. *Biomed Opt Express*. 2019;10(20191105):6084–95. <https://doi.org/10.1364/BOE.10.006084>.
- Mohamed A, Durkee HA, Williams S, et al. Morphometric analysis of in vitro human crystalline lenses using digital shadow photogrammetry. *Exp Eye Res*. 2021;202:108334. <https://doi.org/10.1016/j.exer.2020.108334>.
- Waring GOT, Chang DH, Rocha KM, et al. Correlation of Intraoperative Optical Coherence Tomography of Crystalline Lens Diameter, Thickness, and volume with Biometry and Age. *Am J Ophthalmol*. 2021;225:147–156. <https://doi.org/10.1016/j.ajo.2020.12.021>.
- Jivrajka R, Shammas MC, Boenzi T, et al. Variability of axial length, anterior chamber depth, and lens thickness in the cataractous eye. *J Cataract Refract Surg*. 2008;34:289–94. <https://doi.org/10.1016/j.jcrs.2007.10.015>.

26. Haddad JS, Rocha KM, Yeh K et al. Lens anatomy parameters with intraoperative spectral-domain optical coherence tomography in cataractous eyes. *Clin Ophthalmol* 2019; 13: 253–260. 20190204. <https://doi.org/10.2147/oph.S184208>
27. Meng J, He W, Rong X, et al. Decentration and tilt of plate-haptic multifocal intraocular lenses in myopic eyes. *Eye Vis (Lond)*. 2020;7:17. <https://doi.org/10.1186/s40662-020-00186-3>.
28. Martínez-Enríquez E, Pérez-Merino P, Durán-Poveda S, et al. Estimation of intraocular lens position from full crystalline lens geometry: towards a

new generation of intraocular lens power calculation formulas. *Sci Rep*. 2018;8:9829. <https://doi.org/10.1038/s41598-018-28272-6>.

Publisher's note

Springer Nature remains neutral with regard to jurisdictional claims in published maps and institutional affiliations.